Published in final edited form as:
Science. 2012 August 17; 337(6096): 839–842. doi:10.1126/science.1222826.

Circadian Rhythm of Redox State Regulates Excitability in Suprachiasmatic Nucleus Neurons

Tongfei A. Wang[1,*], **Yanxun V. Yu**[2,*,‡], **Gubbi Govindaiah**[1,3], **Xiaoying Ye**[3,4,ζ], **Liana Artinian**[1,ξ], **Todd P. Coleman**[5], **Jonathan V. Sweedler**[1,2,3,4], **Charles L. Cox**[1,2,3], and **Martha U. Gillette**[1,2,3,6,†]

[1]Department of Molecular and Integrative Physiology, University of Illinois at Urbana-Champaign, Urbana, IL 61801, USA

[2]Neuroscience Program, University of Illinois at Urbana-Champaign, Urbana, IL 61801, USA

[3]Beckman Institute, University of Illinois at Urbana-Champaign, Urbana, IL 61801, USA

[4]Department of Chemistry, University of Illinois at Urbana-Champaign, Urbana, IL 61801, USA

[5]Department of Bioengineering, University of California, San Diego, La Jolla, CA 92093, USA

[6]Department of Cell and Developmental Biology, University of Illinois at Urbana-Champaign, Urbana, IL 61801, USA

Abstract

Daily rhythms of mammalian physiology, metabolism, and behavior parallel the day-night cycle. They are orchestrated by a central circadian clock in the brain, the suprachiasmatic nucleus (SCN). Transcription of clock genes is sensitive to metabolic changes in reduction and oxidation (redox); however, circadian cycles in protein oxidation have been reported in anucleate cells, where no transcription occurs. We tested whether the SCN also expresses redox cycles and how such metabolic oscillations might affect neuronal physiology. We detected self-sustained circadian rhythms of SCN redox state that required the molecular clockwork. The redox oscillation could determine the excitability of SCN neurons through non-transcriptional modulation of multiple K^+ channels. Thus, dynamic regulation of SCN excitability appears to be closely tied to metabolism that engages the clockwork machinery.

Circadian rhythms coordinate body systems and synchronize the internal milieu with daily and seasonal changes in light on Earth. Diurnal changes in the environment generate daily fluctuations in energy availability, to which internal metabolic systems are tuned by self-sustained circadian clocks (1, 2). These near-24 h rhythms emerge from transcriptional-translational feedback loops of core clock genes (3), and oscillations in regulatory cytoplasmic elements, including adenosine 3′,5′-monophosphate (cAMP) (4, 5), Ca^{2+} (6), and activity of protein kinases (7). Superimposed upon circadian rhythms of metabolism are

†To whom correspondence should be addressed. mgillett@illinois.edu.
*These authors contributed equally to this work.
‡Present address: Department of Biology and National Center for Behavioral Genomics, Brandeis University, Waltham, MA 02454, USA
ζPresent address: The SAIC-Frederick, Inc., National Cancer Institute, Frederick, MD 21702
ξPresent address: Department of Biology, Georgia State University, Atlanta, GA 30302-4010

Supplementary Materials
www.sciencemag.org
Materials and Methods
Supplementary Text
Supplementary Figures S1 to S6

near 24-h oscillations due to the contingencies of life. At the cellular level, metabolic state is manifest as redox sate. It is usually described by the homeostasis of reactive free radicals, such as nicotinamide adenine dinucleotide (NAD^+) and flavin adenine dinucleotide (FAD), from reduction-oxidation reactions in metabolism (8). Circadian and energetic cycles are coupled through transcriptional modulation by core clock proteins of genes that regulate metabolism (9, 10), as well as the sensitivity of clock gene transcription to redox state (11–13). However, non-transcriptional interdependency of redox state and neuronal physiology in the circadian context is unexplored.

To test whether redox state exhibits a daily rhythm in the brain's circadian clock, we performed ratiometric redox fluorometry by two-photon laser microscopy of organotypic slices of SCN-bearing rat hypothalamus (14). The relative redox state was measured non-invasively from the ratio of auto-fluorescence emissions in response to 730-nm excitation of two co-factors of cellular metabolism, FAD (500+ nm) and NAD(P)H (400+ nm) (15). We found an endogenous, near-24-h oscillation of redox state in SCN tissue from wild-type rat and mouse (τ = 23.74 ± 0.26 h, τ = 23.75 ± 0.30 h, respectively, χ^2 periodogram analysis, N = 5, Fig. 1A, B, D, E). Application of the oxidizing reagent, diamide (DIA, 5 mM), increased the FAD/NAD(P)H ratio within 2 min ($\Delta F_{500+}/F_{400+}$ = 0.022 ± 0.018 (SEM), $P <$ 0.05, paired Student's t-Test, N = 6, Fig. S1A, B). On the other hand, exposure to a reducing reagent, glutathione (GSH, 1 mM), decreased the ratio ($\Delta F_{500+}/F_{400+}$ = −0.022 ± 0.010, $P <$ 0.01, paired Student's t-Test, N = 6, Fig. S1C). We further evaluated SCN slices from *Bmal1* −/− mice, which lack circadian rhythms (16, 17). *Bmal1* −/− SCNs exhibited stochastic, but not circadian, oscillations in relative redox state (Fig. 1C, F, N = 5). Thus, circadian redox oscillations in rodent SCN require a functional molecular clockwork involving the clock gene, *Bmal1*.

To determine temporal phasing of the SCN redox oscillation, we evaluated two indicators of redox state. First, we examined points across the circadian cycle of SCN brain slices for glutathiolation, the capacity of proteins to incorporate reduced GSH, which binds to available disulfide bonds (18). Glutathiolation peaked in early night, indicating a relatively oxidized state, and was lower in mid-day, reporting a relatively reduced state (Fig. 1G, H, P < 0.05, One-Way ANOVA followed by Tukey's Honestly Significant Difference (HSD) Test, N = 6). We next analyzed the ascorbic acid system, an important antioxidant and neuroprotective buffer in the brain (19). We used capillary electrophoresis with laser-induced fluorescence detection (CE-LIF) to directly measure the concentrations of dehydroascorbic acid (DHA) *vs.* its reduced counterpart, ascorbic acid (AA) (20). Amounts of DHA/AA oscillate with a circadian rhythm, similar to glutathiolation: DHA/AA is highest in early night and lowest in midday (Fig. 1I, $P <$ 0.05, test as above, N = 3). Parallel changes in these distinct redox systems confirm circadian oscillation of global redox state in rat SCN, with a significantly oxidized state in early night *vs.* reduced state during daytime. These results support and extend the redox oscillation found in peripheral tissue (21, 22) to the central circadian clock in the brain.

To assess possible relations between the circadian oscillations of redox state and neuronal physiology, we evaluated membrane excitability in rat SCN neurons by examining resting membrane potential (V_m), input resistance (R_{in}), and spontaneous action potentials (SAP). Recording from current-clamped neurons, we observed circadian oscillations of V_m (Fig. 2A, N = 364; Fig. 2B, N = 36–60 at 5 circadian times (CTs) around the free-running clock cycle, $P <$ 0.001, test as above), R_{in} (Fig. 2C, N = 337; Fig. 2D, N = 15–30, $P <$ 0.05, test as above), frequency of SAP (Fig. S2A, N = 334), and percentage of neurons discharging SAP (active, Fig. S2C, N = 334) (15). These data from rat exhibit a similar circadian pattern in membrane excitability as from mouse (23). Comparing circadian oscillations of redox state (Fig. 1H, I) with V_m in SCN neurons (Fig. 2B) revealed that the daytime reduced state

matched the depolarized V_m, whereas the oxidized state of subjective night aligned with hyperpolarized V_m.

To probe potential interdependency of redox state and neuronal excitability, we tested effects of pharmacological redox manipulation on V_m of SCN neurons at various CTs. The oxidizing reagent, DIA, hyperpolarized V_m in a reversible manner (Fig. 2E, −8.68 ± 0.64 mV, mean around circadian cycle, $N = 104$); in contrast, exposure to the reducing reagent, GSH, caused depolarization (Fig. 2G, +10.67 ± 1.03 mV, $N = 97$). Similar results were obtained from current-clamp recording with redox reagents in the patch pipette (Fig. S4). Exogenous redox regulation of V_m in SCN depends on CT: both drugs caused maximal effects near subjective dusk (CT 10 – 12), and minimal effects near subjective dawn (CT 0 – 2, Fig. 2I, $P < 0.01$, test as above, $N = 10–20$). Shifts in V_m caused by redox manipulation were associated with changes of R_{in}. Based upon the slopes of current-voltage (I–V) curves constructed before and during redox treatment, DIA was found to decrease the R_{in} of SCN neurons by 364 ± 30 MΩ (48.83%, Fig. 2F, J, $N = 41$), whereas GSH increased R_{in} by 64 ± 11 MΩ (10.81%, Fig. 2H, J, $N = 36$). Percentage changes in R_{in} were not correlated with changes in V_m (Fig. S5, $P > 0.05$, Linear Correlation and Regression, $N = 37–42$) and were independent of CT (Fig. 2J, $P > 0.05$, One-Way ANOVA, $N = 5–9$). Redox-induced changes in membrane properties were rapid, occurring in < 2 min (68.7 ± 10.6 s).

To identify potential targets for redox regulation of neuronal excitability, we gradually changed command voltages from −50 to −110 mV (6-s duration) on voltage-clamped SCN neurons between CT 9–13. By comparing membrane currents before and during exposure to the redox reagents, we examined the voltage-dependency of target ion channel(s). Bath application of DIA elicited a strong outward current (100.1 ± 22.8 pA at −50 mV, $N = 6$, Fig. 3A, B, C, G), associated with an increased conductance as indicated by a greater slope of the current response to the ramped voltage command. The I–V relationship before and during DIA treatment revealed a reversal potential at −81.4 ± 7.0 mV and conductance increases of 154.9 ± 22.5 % (Fig. 3B, H). Thus, DIA appears to act through an outward-rectifier K^+ channel(s) (Fig. 3C). We confirmed this prediction by replacing K^+ with Cs^+, a general K^+-channel blocker, in the recording pipette. Under this condition, the DIA-evoked outward current was significantly attenuated (−1.6 ± 1.2 pA at −50 mV, $P < 0.01$, Tukey's HSD Test, $N = 6$, Fig. 3D through G). Only small conductance changes could be detected during DIA treatment (14.2 ± 4.7 %, Fig. 3E, H). Exposure to GSH elicited an inward current in SCN neurons (−40.6 ± 8.5 pA at −50 mV, $N = 6$, Fig. 3G), with a reversal potential at −79.9 ± 4.0 mV and a conductance change of −38.2 ± 6.3 % (Fig. 3H). The GSH-evoked inward current was attenuated by Cs^+ in the internal solution, as well (−7.9 ± 2.1 pA at −50 mV, 34.1 ± 16.8 % conductance changes, $P < 0.01$, test as above, $N = 6$, Fig. 3G, H), also supporting the involvement of K^+ currents.

To explore the potential role of leak K^+ channels in redox regulation, we applied a specific blocker of this channel, bupivacaine (Bupi, 100 μM). In the presence of Bupi, DIA induced an outward current of 31.9 ± 4.4 pA at −50 mV (Fig. 3G, $N = 5$), with conductance changes of 70.4 ± 11.2% (Fig. 3H, $N = 5$), but amplitudes were lower than those in control media (Fig. 3G, H, $P < 0.05$, test as above). Bupi attenuated GSH-induced inward current and conductance changes, as well (−40.6 ± 8.5 pA at −50 mV, 11.0 ± 12.4%, $P < 0.05$, test as above, $N = 5$, Fig. 3G, H). These results support the leak K^+ channel as a target of redox regulation.

We further used voltage-step commands to examine the possibility that redox state regulates voltage-gated K^+ channels (Fig. 4A through C, (15)). We found that DIA significantly enhanced the transient peak of the outward current induced by −10 mV steps (288.4 ± 36.5 pA, $N = 5$, Fig. 4D and G). This enhancement was completely abolished by 4-aminopyridine

(4-AP, 5 mM), a selective inhibitor of A-type K^+ channel (−11.7 ± 17.2 pA, $P < 0.01$, test as above, $N = 6$, Fig. 4E, G), but was insensitive to tetraethylammonium (TEA, 20 mM), a delayed rectifier K^+-channel blocker (282.4 ± 34.7 pA, $P > 0.05$, test as above, $N = 6$, Fig. 4F, G). The persistent outward current was insensitive to DIA treatment with or without 4-AP or TEA ($P > 0.05$, One-Way ANOVA, $N = 5 – 6$, Fig. 4H). On the other hand, GSH suppressed the transient peak of the outward current (−149.5 ± 37.3 pA, $N = 5$, Fig. 4G); similar to DIA, the suppression was sensitive to 4-AP (6.8 ± 14.3 pA, $P < 0.01$, Tukey's HSD Test, $N = 5$, Fig. 4G), but not TEA (−164.8 ± 25.4 pA, $P > 0.05$, test as above, $N = 6$, Fig. 4G), while the persistent outward current was not affected by any drug ($P > 0.05$, One-Way ANOVA, $N = 5 – 6$, Fig. 4H). These results support the involvement of a 4-AP-sensitive voltage-gated K^+ channel in redox regulation.

The daily rhythm of electrical activity in the SCN is essential for the functionality of the central pacemaker in synchronizing the body clocks (24, 25); several K^+ channels have been identified underlying the changing excitability (26–28). We found a redox regulation of K^+ conductance underwent circadian changes in SCN neurons, with characteristics of both leak and A-type K^+ channels. This provides a non-transcriptional pathway for the metabolic cycle to engage the clockwork machinery (Fig. S6). Energetic fluctuation in the central nervous system has been considered to be a consequence of neuronal activity. However, our study implies that changes in cellular metabolic state could be the *cause*, rather than the *result*, of neuronal activity. Crosstalk between energetic and neuronal states bridges cellular state to systems physiology.

Supplementary Material

Refer to Web version on PubMed Central for supplementary material.

Acknowledgments

We thank S.-H. Tyan for insightful discussions at the inception of this work; G. Robinson, R. Gillette and J.M. Mitchell for critical feedback; J.M. Ding and G.F. Buchanan for data support; K.E. Weis and J.M. Arnold for technical support; S.C. Liu for data analysis consultation and M.C. Holtz for manuscript preparation. Research was supported by the National Heart, Lung and Blood Institute (RO1HL092571 Z ARRA, RO1HL086870) to MUG, by National Eye Institute (EY014024) to CLC, by the National Institute on Drug Abuse (P30DA018310) to JVS and the National Science Foundation (CHE 11-11705 to JVS and CCF09-39370 to TPC). Content is solely the responsibility of the authors and does not necessarily represent the official views of the NIH or NSF.

References and Notes

1. Green CB, Takahashi JS, Bass J. The meter of metabolism. Cell. 2008; 134:728. [PubMed: 18775307]
2. Bass J, Takahashi JS. Circadian integration of metabolism and energetics. Science. 2010; 330:1349. [PubMed: 21127246]
3. Lowrey PL, Takahashi JS. Mammalian circadian biology: elucidating genome-wide levels of temporal organization. Annu Rev Genomics Hum Genet. 2004; 5:407. [PubMed: 15485355]
4. Prosser RA, Gillette MU. Cyclic changes in cAMP concentration and phosphodiesterase activity in a mammalian circadian clock studied in vitro. Brain Res. 1991; 568:185. [PubMed: 1667616]
5. O'Neill JS, Maywood ES, Chesham JE, Takahashi JS, Hastings MH. cAMP-dependent signaling as a core component of the mammalian circadian pacemaker. Science. 2008; 320:949. [PubMed: 18487196]
6. Harrisingh MC, Wu Y, Lnenicka GA, Nitabach MN. Intracellular Ca2+ regulates free-running circadian clock oscillation in vivo. J Neurosci. 2007; 27:12489. [PubMed: 18003827]
7. Robles MS, Boyault C, Knutti D, Padmanabhan K, Weitz CJ. Identification of RACK1 and protein kinase Calpha as integral components of the mammalian circadian clock. Science. 2010; 327:463. [PubMed: 20093473]

8. Droge W. Free radicals in the physiological control of cell function. Physiol Rev. 2002; 82:47. [PubMed: 11773609]
9. Turek FW, et al. Obesity and metabolic syndrome in circadian Clock mutant mice. Science. 2005; 308:1043. [PubMed: 15845877]
10. Marcheva B, et al. Disruption of the clock components CLOCK and BMAL1 leads to hypoinsulinaemia and diabetes. Nature. 2010; 466:627. [PubMed: 20562852]
11. Rutter J, Reick M, Wu LC, McKnight SL. Regulation of clock and NPAS2 DNA binding by the redox state of NAD cofactors. Science. 2001; 293:510. [PubMed: 11441146]
12. Dioum EM, et al. NPAS2: a gas-responsive transcription factor. Science. 2002; 298:2385. [PubMed: 12446832]
13. Rutter J, Reick M, McKnight SL. Metabolism and the control of circadian rhythms. Annu Rev Biochem. 2002; 71:307. [PubMed: 12045099]
14. Huang S, Heikal AA, Webb WW. Two-photon fluorescence spectroscopy and microscopy of NAD(P)H and flavoprotein. Biophys J. 2002; 82:2811. [PubMed: 11964266]
15. Materials and Methods, Supplementary Text and Supplementary Figures are available as Supplementary Materials on *Science* Online.
16. Bunger MK, et al. Mop3 is an essential component of the master circadian pacemaker in mammals. Cell. 2000; 103:1009. [PubMed: 11163178]
17. Ko CH, et al. Emergence of noise-induced oscillations in the central circadian pacemaker. PLoS Biol. 2010; 8:e1000513. [PubMed: 20967239]
18. Sullivan DM, Levine RL, Finkel T. Detection and affinity purification of oxidant-sensitive proteins using biotinylated glutathione ethyl ester. Methods Enzymol. 2002; 353:101. [PubMed: 12078486]
19. Rice ME. Ascorbate regulation and its neuroprotective role in the brain. Trends Neurosci. 2000; 23:209. [PubMed: 10782126]
20. Kim WS, Dahlgren RL, Moroz LL, Sweedler JV. Ascorbic acid assays of individual neurons and neuronal tissues using capillary electrophoresis with laser-induced fluorescence detection. Anal Chem. 2002; 74:5614. [PubMed: 12433096]
21. O'Neill JS, Reddy AB. Circadian clocks in human red blood cells. Nature. 2011; 469:498. [PubMed: 21270888]
22. O'Neill JS, et al. Circadian rhythms persist without transcription in a eukaryote. Nature. 2011; 469:554. [PubMed: 21270895]
23. Belle MD, Diekman CO, Forger DB, Piggins HD. Daily electrical silencing in the mammalian circadian clock. Science. 2009; 326:281. [PubMed: 19815775]
24. Brown TM, Piggins HD. Electrophysiology of the suprachiasmatic circadian clock. Prog Neurobiol. 2007; 82:229. [PubMed: 17646042]
25. Golombek DA, Rosenstein RE. Physiology of circadian entrainment. Physiol Rev. 2010; 90:1063. [PubMed: 20664079]
26. Itri JN, Michel S, Vansteensel MJ, Meijer JH, Colwell CS. Fast delayed rectifier potassium current is required for circadian neural activity. Nat Neurosci. 2005; 8:650. [PubMed: 15852012]
27. De Jeu M, Geurtsen A, Pennartz C. A Ba(2+)-sensitive K(+) current contributes to the resting membrane potential of neurons in rat suprachiasmatic nucleus. J Neurophysiol. 2002; 88:869. [PubMed: 12163538]
28. Itri JN, et al. Circadian regulation of A-type potassium currents in the suprachiasmatic nucleus. J Neurophysiol. 2010; 103:632. [PubMed: 19939959]

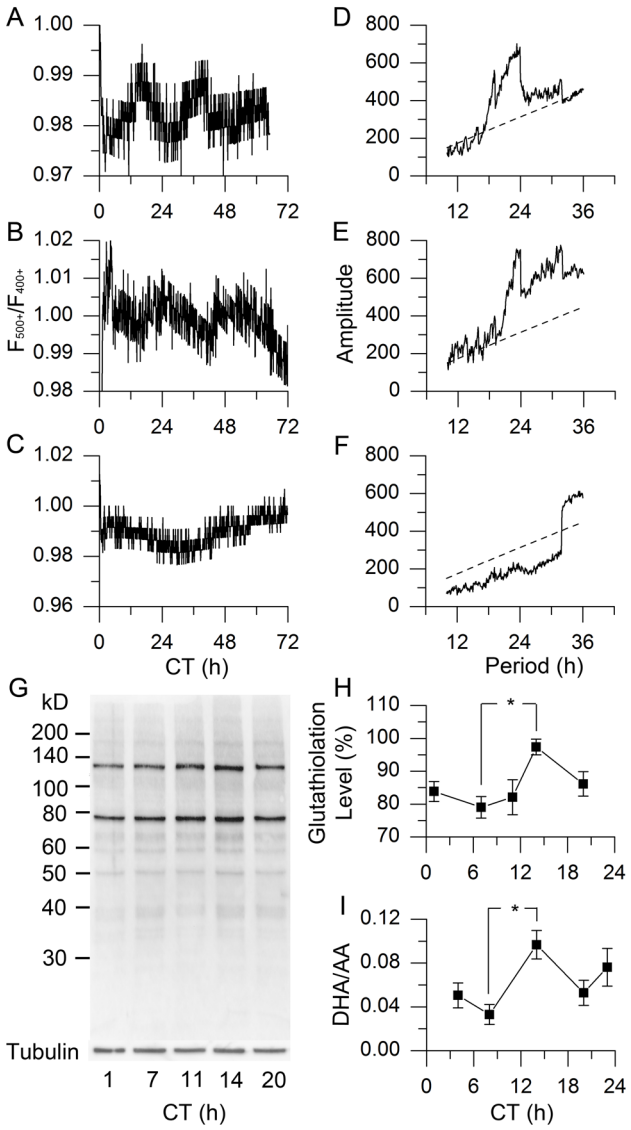

Fig. 1.

Circadian oscillation of redox state in rodent SCN. **(A–C)** Real-time imaging of relative redox state in SCN of wild-type (WT) rat (A), WT mouse (B) and *Bmal1* −/− mouse (C). **(D–F)** χ^2 periodograms (solid) of redox oscillations in SCN of WT rat (D), WT mouse (E), and *Bmal1* −/− mouse (F), based on data in A–C, respectively, with the confidence interval of 0.001 (dashed); τ_{rat} = 23.74 ± 0.26 h (mean ± SD), τ_{mouse} = 23.75 ± 0.30 h; N = 5 for each group. **(G)** Glutathiolation patterns of BioGEE incorporation into rat SCN tissue over 5 points of circadian time (CT, which has a free-running time-base driven by the endogenous clock). **(H)** Protein glutathiolation over 5 CTs in rat SCN (P < 0.05, One-Way ANOVA; *, P < 0.05, Tukey's Honestly Significant Difference (HSD) Test; N = 6). **(I)** DHA/AA ratio in rat SCN over 5 CTs (P < 0.05, One-Way ANOVA; *, P < 0.05, Tukey's HSD Test; N = 3).

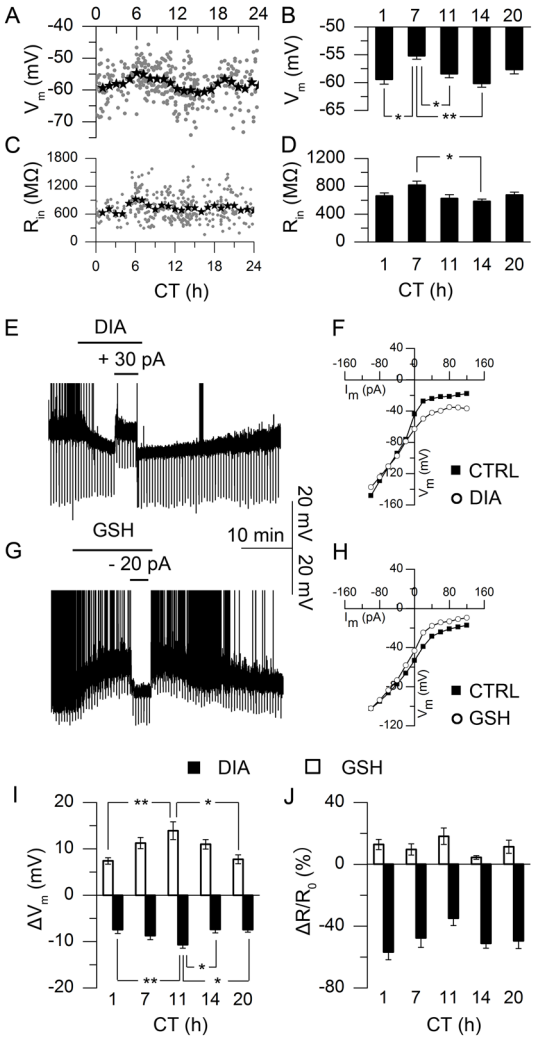

Fig. 2.

Circadian oscillations of neuronal excitability and redox regulation in rat SCN neurons. **(A)** Individual neurons (grey dots, 2-min recording, $N = 364$) and 1-h averages (star) of membrane potential (V_m). **(B)** V_m means at 5 CTs ($P < 0.001$, One-Way ANOVA; **, $P < 0.01$, *, $P < 0.05$, Tukey's HSD Test; $N = 36–60$). **(C)** Membrane input resistance (R_{in}) measured by hyperpolarizing current steps ($N = 337$). **(D)** Average R_{in} from I–V constructed by current steps from −100 to +120 pA (20 pA increments, 800 ms duration) at 5 CTs ($P < 0.05$, One-Way ANOVA; *, $P < 0.05$, Tukey's HSD Test; $N = 15–30$). **(E, G)** Current-clamp recording of V_m in response to oxidizing (E, diamide, DIA, 5 mM) or reducing reagent (G, glutathione, GSH, 1 mM), truncated spontaneous action potentials (SAP). **(F, H)** I–V curve before (filled) and during (open) DIA (F) or GSH (H) treatment. **(I)** Redox-induced ΔV_m at 5 CTs ($P < 0.01$, One-Way ANOVA; **, $P < 0.01$, *, $P < 0.05$, Tukey's HSD Test; $N = 10–20$). **(J)** Redox-induced $\Delta R_{in}/R_{in0}$% at 5 CTs ($P > 0.05$, One-Way ANOVA; $N = 5–9$).

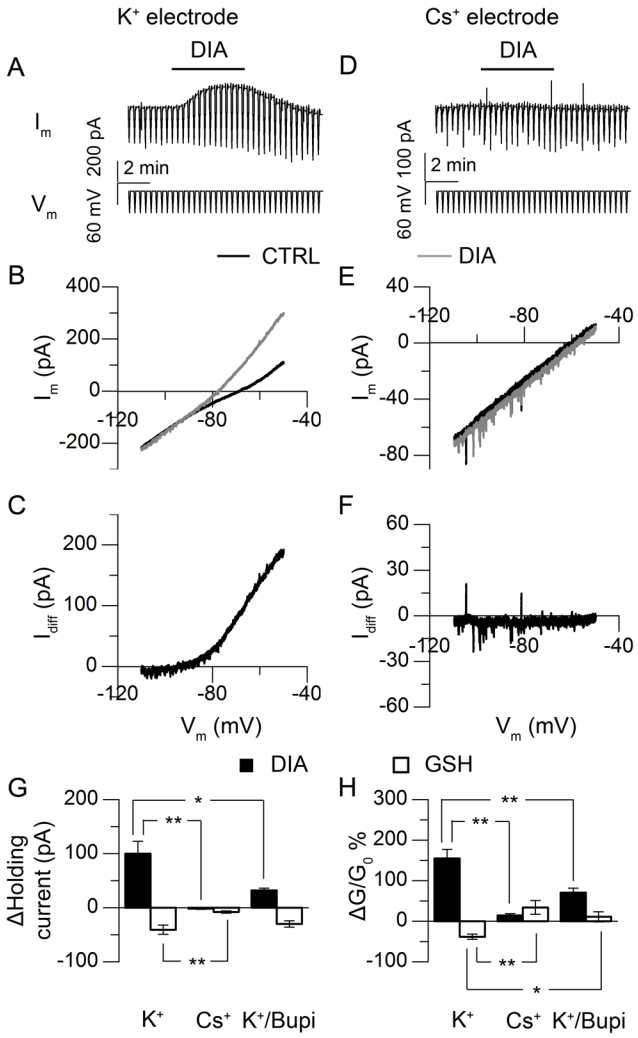

Fig. 3.

Redox regulation of neuronal excitability through K^+ current (CT 9–13). **(A)** Voltage-clamp recording of SCN neuron, with repeating slow-ramped voltage commands from −50 mV to −110 mV. **(B)** I–V curve constructed based on the command voltage and membrane current recorded, before (black) and during (grey) DIA treatment. **(C)** The DIA-evoked current as calculated from the difference in the membrane response in (B). **(D–F)** Similar voltage clamp recordings as (A–C), except that Cs^+ replaced K^+ in the patch pipette. **(G, H)** Holding current (G) and conductance (H) changes induced by redox reagents (DIA, black; GSH, white) with electrodes containing K^+ ($P < 0.01$, paired Student's *t*-Test to control; $N = 6$), Cs^+ ($P > 0.05$ (current), $P < 0.01$ (conductance) for DIA, $P < 0.05$ for GSH, paired Student's *t*-Test to control; $N = 6$), or K^+ (in electrode) with bupivacaine (Bupi, 100 μM) in bath ($P < 0.01$, paired Student's *t*-Test to control; $N = 5$); for the comparison across groups, $P < 0.01$, One-Way ANOVA; **, $P < 0.01$, *, $P < 0.05$, Tukey's HSD Test.

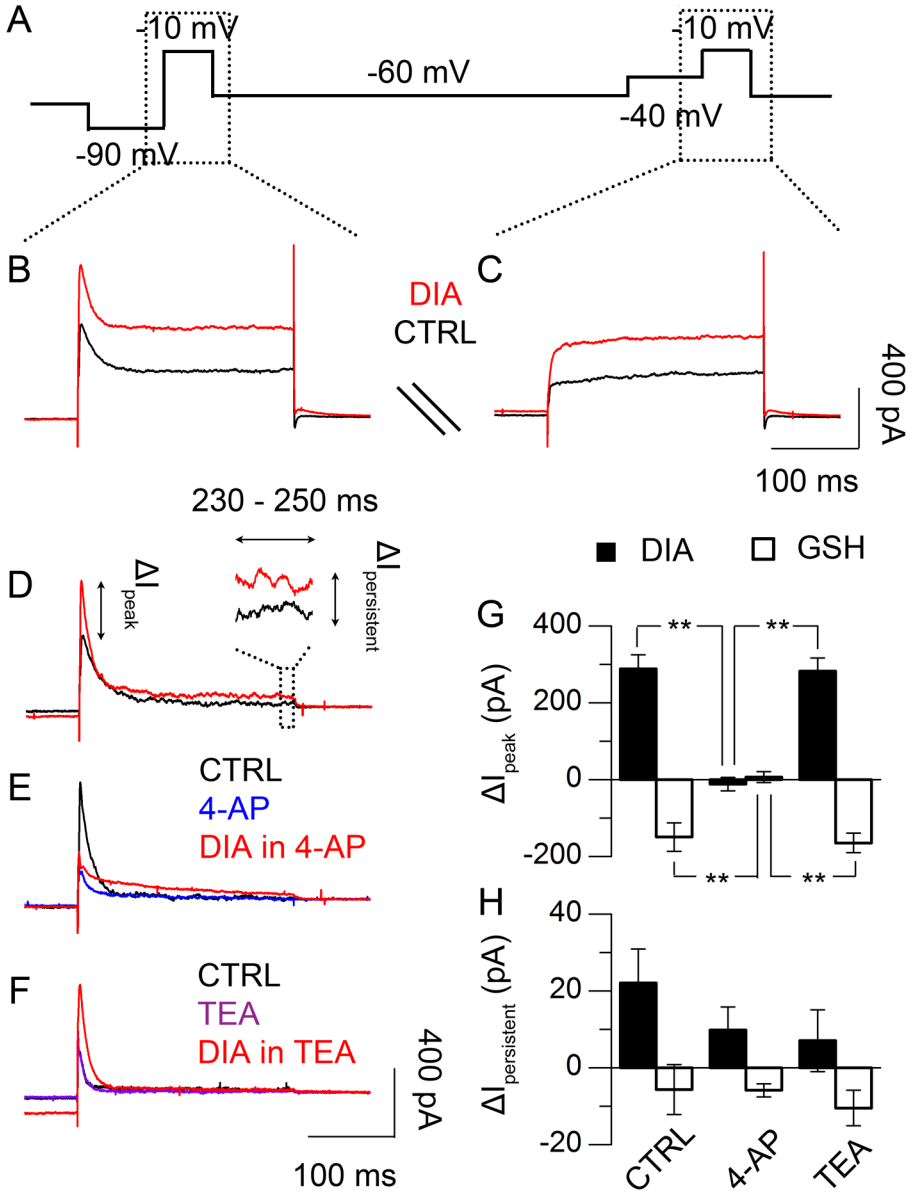

Fig. 4.

Redox regulation of voltage-dependent K^+ currents (CT 9 – 13). **(A)** Recording protocol of repeating voltage-step commands to voltage-clamped SCN neurons (15), before, during, and after drug treatment. **(B, C)** Current responses to the voltage-step commands of −10 mV pulses, following either −90 mV (B) or −40 mV (C) pre-pulse, before (black) or during (red) DIA treatment. **(D)** Voltage-dependent outward current in response to −10 mV voltage-step stimulation, calculated from the difference between the current responses in (B) and (C). **(E, F)** Effects of 4-aminopyridine (4-AP, 5 mM) and tetraethylammonium (TEA, 20 mM) on outward current evoked by DIA. **(G)** Transient current (< 10 ms) changes in response to redox treatment (DIA, black; GSH, white), with or without 4-AP or TEA ($P < 0.01$, One-Way ANOVA; **, $P < 0.01$, Tukey's HSD Test; $N = 5–6$). **(H)** Persistent current (230–250 ms) changes in response to redox treatment, with/without 4-AP or TEA ($P > 0.05$, One-Way ANOVA; $N = 5–6$).